Investigation of potential oscillations and ion energy distribution function near the hollow cathode

Yu. Qin[1], Kan. Xie[2], Zun Zhang[3] and JiTing. Ouyang[4]

Beijing Institute of Technology, Beijing, 100081, China

Ning Guo[5], Zengjie Gu[6]

National key laboratory of Science and Technology on Vacuum Technology &Physics, Lanzhou 730000, China

Abstract: The potential oscillations near the hollow cathode are experimentally investigated. An emissive probe is employed to measure the waveforms of potential oscillations in the cathode plume. The potential oscillations frequency and amplitude spectrum of the potential oscillations from FFT are analyzed. At low current, the potential oscillations concentrated on the ionization-like instabilities with characteristics of low frequency and high amplitude. At high current, the potential oscillations frequency increased and the high frequency potential oscillations appears which is driven by ion acoustic turbulence with characteristics of high frequency and low amplitude. The onset of ion acoustic turbulence is observed as current increased. The ion energy distribution function by numerical simulation was also investigated. The results show that the ion energy increased as the amplitude of plasma potential oscillation and the frequency of plasma potential oscillation increased.

Nomenclature

T_i = ion temperature
T_e = electron temperature

[1]Doctoral student, Beijing Institute of Technology, qinyu@bit.edu.cn.

[2] Associate professor, corresponding author, Beijing Institute of Technology, xiekan@bit.edu.cn.

[3] Postdoctoral, Beijing Institute of Technology, zhangzun@bit.edu.cn.

[4] Professor, Beijing Institute of Technology, jtouyang@bit.edu.cn.

[5]Researcher, National key laboratory of Science and Technology on Vacuum Technology &Physics, guoningaa@163.com

[6]Master student, National key laboratory of Science and Technology on Vacuum Technology &Physics, guzengjie@foxmail.com

V_e = electron drift velocity

I. Introduction

Hollow cathodes have been studied widely due to their extensive ranges in application especially in electric propulsion systems, such as ion thrusters, Hall thrusters and cathodic plasma contactor [1-4]. Hollow cathodes become critical components in propulsion system and one of the life limiting factors of cathode failure is the erosion from high energy ion bombardment [5]. In both Hall thrusters and ion thrusters, there exists an unstable discharge phenomenon in which the discharge voltage oscillates [6]. The discharge voltage oscillations produce high-energy ions in the cathode plumes with energy significantly in excess of the discharge voltage and these high energy ions cause higher erosion rates than the anticipated erosion rates that are observed in some tests. Goebel *et al.* observed large amplitude plasma potential oscillations nearby a hollow cathode at some operating conditions and reported that ions with energies significantly in excess of the discharge voltage have been found in high current hollow cathode discharges [7, 8]. The potential fluctuations can exceed five times T_e, suggesting that turbulent acoustic oscillations (0.1–2 MHz) and/or ionization instabilities (40–150 kHz) exist under certain conditions near the cathode/keeper exit. Ions generated in this region at the peak of the plasma potential fluctuations acquire a large energy as they leave the plasma and strike the cathode electrodes and anode wall, which causes the significant sputtering of the surfaces near the cathode plume. The variation in the magnitude of the potential fluctuations and the change in the characteristics and location of the unstable region of the plasma ball as the discharge parameters and geometry change likely explain the different erosion rates and locations observed in different experiments [9]

The ionization instabilities in moderately high ionization fraction plasmas like these are sometimes called predator-prey oscillations, in that the ionization tends to deplete the local neutral gas, which causes the density to drop and reduce the discharge current-carrying plasma density. The system then oscillates on the ionization-rate time scales [10, 11], depending on the physical lengths and size of the discharge components. The oscillations occur at the characteristic with low frequency for operating condition, and show that cathode emission current and plasma density oscillations in the cathode plume are strongly correlated. This behavior is modulated on the ionization rate and neutral gas fill time constants.

The ion acoustic instability is an electrostatic mode that naturally arises in plasmas where there is a large disparity in ion and electron temperatures: $T_e / T_i >> 1$ and where there is a significant electron drift velocity V_e [12]. These are usually oscillations in the frequency range with small to moderate

amplitudes that vary continuously from fractions of a volt on the electrodes in the spot mode to tens of volts on the electrodes into the plume mode. Mikellides et al. showed that the electron Mach number and electron to ion temperature ratio were high enough in the orifice and near-plume plasma to onset ion acoustic turbulence (IAT)—a mode commonly found in current-carrying plasmas and often associated with significant anomalous collisionality. Later they found the IAT exists in the hollow cathode plume and the IAT amplitude at first decreases and then increases with discharge current at fixed flow rate. It decreases with flow rate at fixed discharge current. IAT can transfer its energy to plasma ions through collisionless processes such as ion Landau damping. This process in turn can lead to the formation of energetic ion tails. In their most recent work, they directly measured the IAT in a 100-A LaB6 cathode, and they demonstrated at low flow rate a correlation between the amplitude of IAT turbulence and the growth of a high energy ion tail in the plasma. This observation supported the idea that energetic ions and the IAT are linked in the cathode plume [13, 14]. Both the low frequency ionization-like instabilities and high frequency ion acoustic turbulence instabilities can work to generate high energy ions.

Here, the waveforms of potential oscillations near the hollow cathode of an ion thruster were measured by using an emissive probe. The potential oscillations frequency, amplitude spectrum of the potential oscillations from FFT, and ion energy distribution function by numerical simulation were investigated. The potential oscillations frequency ranged from low frequency ionization-like instabilities to high frequency ion acoustic turbulence instabilities which depend on the discharge current. The ion energy increased as the amplitude of plasma potential oscillation and the frequency of plasma potential oscillation increased by numerical simulation.

II. Experimental set-up

The experimental set-up consists vacuum facility, discharge chamber configuration and diagnostic tools is same to ones used elsewhere [6]. Briefly, this test was performed in a 1.8 m diameter by 4 m long stainless steel vacuum chamber that was pumped with a diffusion pump. The working vacuum pressure was in the range of 10^{-4} to 10^{-3}Pa corresponding to typical xenon flow rates of 1 to 15 sccm. The discharge chamber configuration is shown in Fig. 1. The hollow cathode was a 6 mm diameter tube which was capped with an orifice plate that had a 0.6 mm diameter orifice on its centreline. The cathode tube and insert were heated by a resistive coil wrapped around the outside of the tube, which was insulated by a multiple-layer, tantalum-foil radiation shield. The keeper orifice plate had a 2.4 mm

diameter orifice positioned about 1 mm downstream of the cathode orifice plate. Measurements of potential oscillations were performed using an emissive probe.

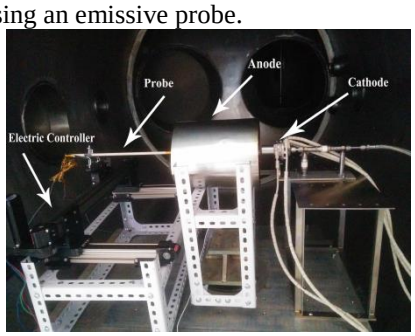

Figure 1 Discharge chamber configuration of ring-type anode

III. Experimental results and discussion

Figure 2 shows the detection region where the emissive probe measurements were made and also shows the configurations of the hollow cathode. Here, the gap relative to the hollow cathode orifice is 0.5 cm, and the detection region is 7.5 cm in width and 15 cm in length. At each operating condition, the xenon flow rate and discharge current were held constant and the discharge voltage was allowed to adjust to a steady-state value. The xenon mass flux rate was contorted by SLA5800 Series mass flow meters and mass flow controllers of BROOKS INSTRUMENTS, and its flow accuracy is about 0.9%.

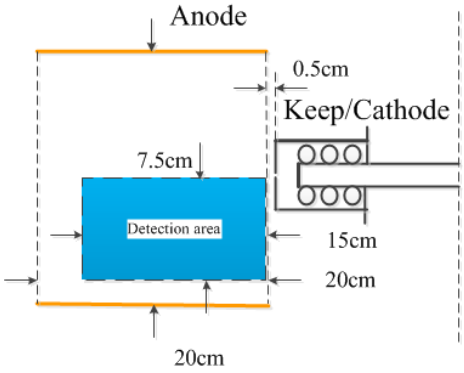

Figure 2. Test regions for emissive probe measurements for ring-type anode configuration

Figure 3 shows average potential profiles and amplitude of plasma potential measurements for the ring-type anode configuration under the following operating conditions: (a) J_D = 3 A, V_D =42 V, flow =2.5 sccm, (*b*) J_D = 5 A, V_D = 66 V, flow =2.5 sccm, and (c) J_D = 9 A, V_D = 24.3 V, flow =7.5 sccm, respectively. We can see from the average plasma potential profile that there was a potential well at the cathode orifice and a potential hill just downstream of the hollow cathode. As the discharge current and flow rate increased, the potential hill was more obvious.

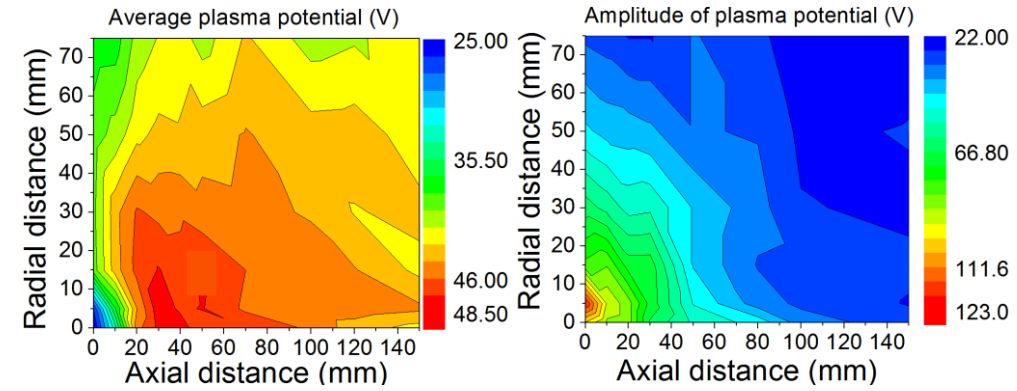

(a) J_D = 3 A, V_D =42 V, flow = 2.5 sccm

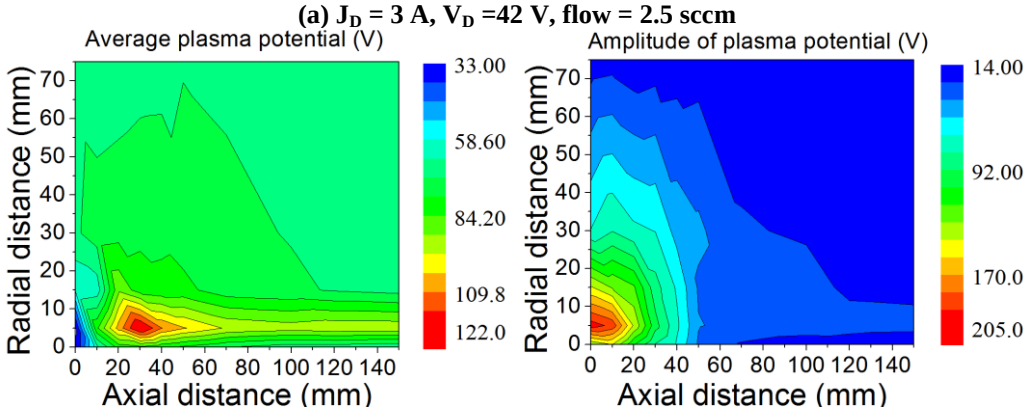

(*b*) J_D = 5 A, V_D = 66 V, flow =2.5 sccm

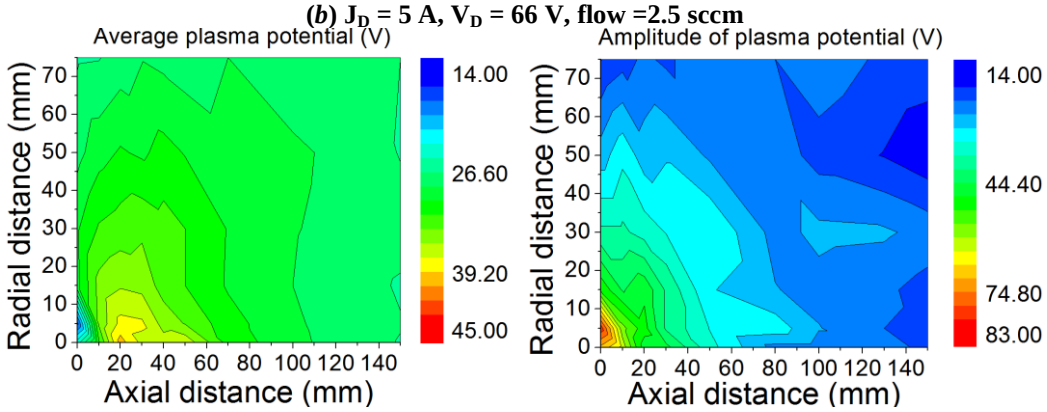

(c) J_D = 9 A, V_D = 24.3 V, flow =7.5 sccm

Figure 3. Emissive probe of average plasma potential measurements and amplitude of plasma potential measurements for: (a) J_D = 3 A, V_D = 42 V, flow = 2.5 sccm, condition (*b*) J_D = 5 A, V_D = 66 V, flow = 2.5 sccm, and condition (c) J_D = 9 A, V_D = 24.3 V, flow = 7.5 sccm for the ring-type anode.

To measure the waveform of the plasma potential, the emissive probe was connected to an oscilloscope (Tektronik DPO 4104B), sampling at a rate of 100 MHz, to monitor the time- resolved plasma potentials.

Certain locations were chosen for the plasma oscillation measurements as shown in Figure 4 (black circles), correspond to r = 0 mm and z = 0, 10 and 20 mm relative to the keeper orifice. Figure 5

shows the resulting potential waveforms at certain location for test conditions: R5a J_D = 5A, V_D = 66 V, flow = 2.5 sccm and R9c J_D = 9 A, V_D = 24.3 V, flow = 7.5 sccm.

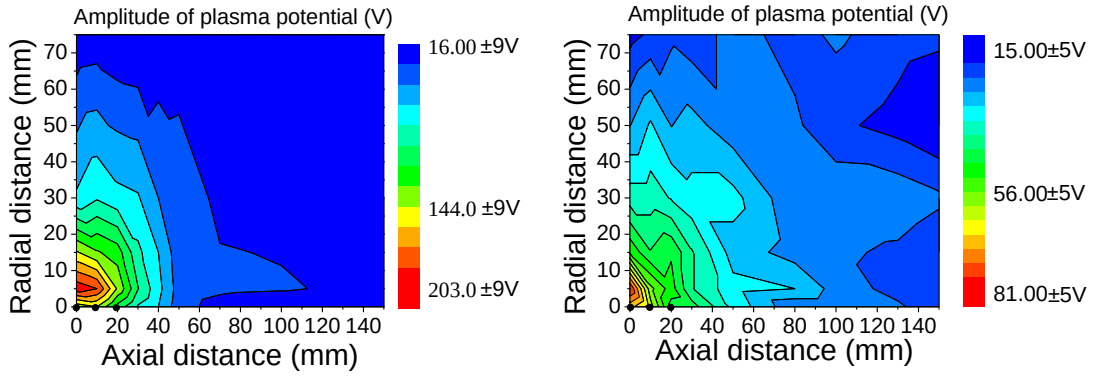

Figure 5.Emissive probe of amplitude of plasma potential measurements under condition: J_D = 5 A, V_D = 66 V, flow = 2.5 sccm and J_D = 9 A, V_D = 24.3 V, flow = 7.5 sccm for a ring-type anode. Black circles denote temporal plasma potential waveforms measurements locations.

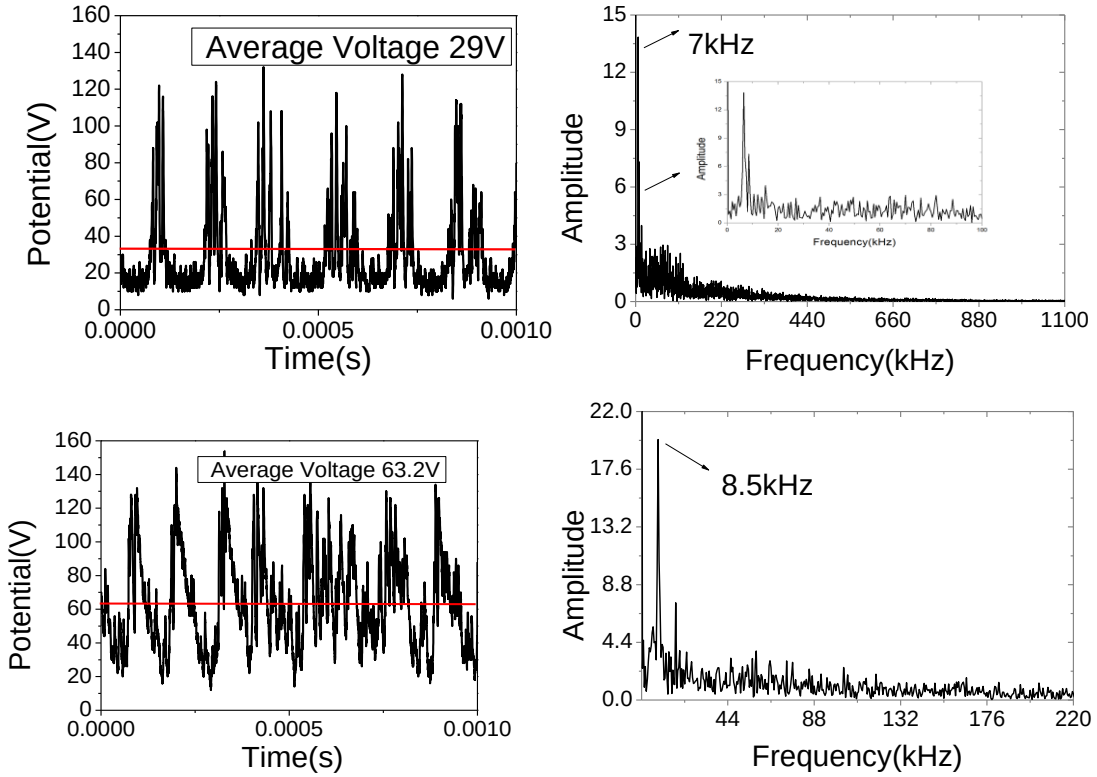

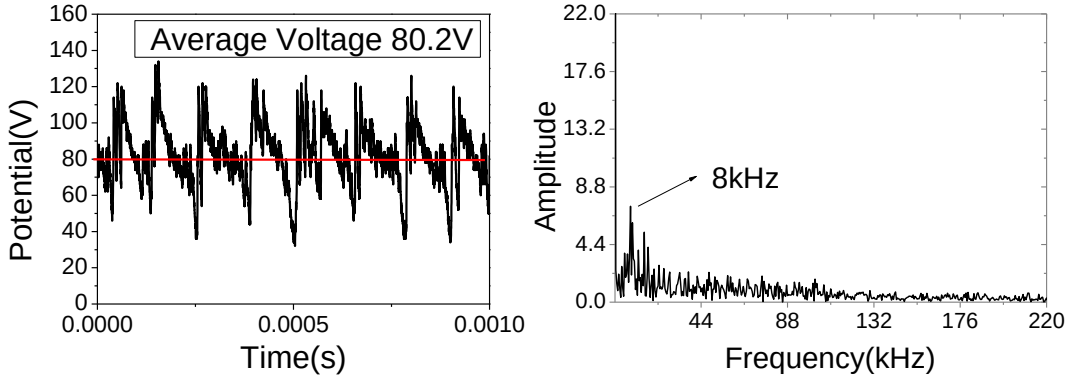

（a）**R5a J_D = 5A, V_D = 66 V, flow = 2.5 sccm**

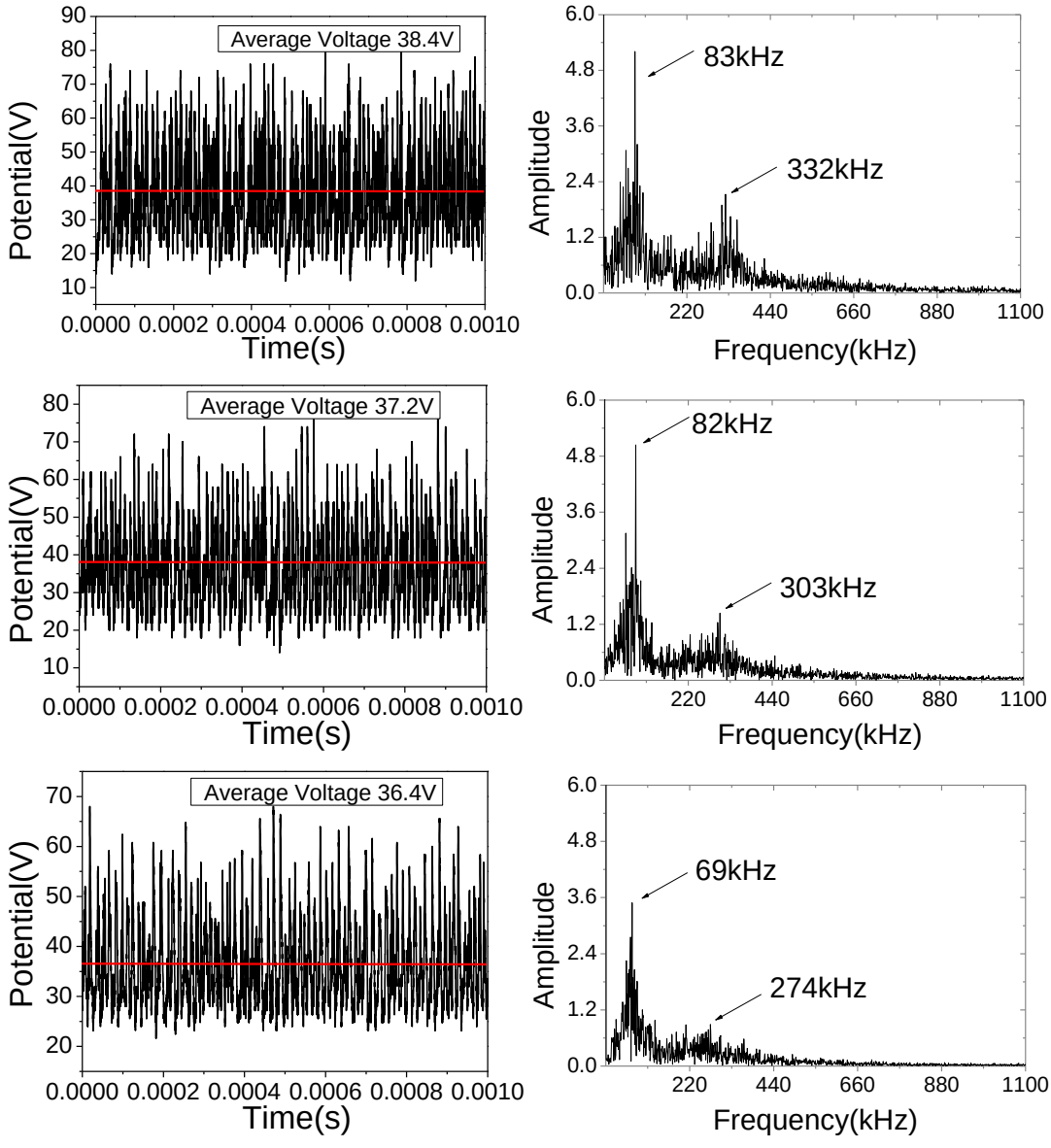

（b）**R9c J_D = 9 A, V_D = 24.3 V, flow = 7.5 sccm.**

Figure 5 the waveforms of potential oscillations and the corresponding amplitude spectrum from FFT at certain locations for test conditions: (a)R5a J_D = 5A, V_D = 66 V, flow = 2.5 sccm and (b)R9c J_D = 9 A, V_D = 24.3 V, flow = 7.5 sccm.

In fig. 5(a) the main oscillations frequency is range from 7 kHz to 10 kHz which is driven by ionization instabilities. The amplitude of this kind of potential oscillations is relative large. In fig. 5(b) the main oscillations frequency consists of two parts, one is range from 70 kHz to 85 kHz which is also driven by ionization instabilities and another is range from 200 kHz to 332 kHz which is driven by ion acoustic turbulence. In this case, the amplitude of potential oscillations which caused by ionization instabilities is larger than the amplitude of potential oscillations which caused by ion acoustic turbulence.

IV. Numerical model

The model described below takes the directly measured plasma properties as inputs and generates a resulting Ion Energy Distribution Function (IEDF).

In numerical model, only ions are considered and the movement of ions is tread using a particle–in-cell (PIC) method for transporting the ions in electrostatic fields. The movement can be given by:

$$\frac{\mathrm{d}}{\mathrm{d}t} m\mathbf{v} = q\left(\mathbf{E} + \mathbf{v} \times \mathbf{B}\right) \tag{1}$$

$$\frac{\mathrm{d}}{\mathrm{d}t} \mathbf{x} = \mathbf{v} \tag{2}$$

Where m is the mass of an ion, $\boldsymbol{E}$ is the electric field, $\boldsymbol{B}$ is the magnetic field, q is electronic charge, x is the position vector and v is the ion velocity vector.

According to the laboratory test potential hill structure and potential hill theory, the internal ionization efficiency in the small hole of the hollow cathode is generally less, that is, major ionization events occurred in the ionization chamber was the most important mechanism by which charge generation took place. Thus we throw the ion at the place where the potential is at its highest. The electron and neutral gas can influence collision ionization, charge exchange reaction rates that could alter the resulting IEDF, but for this simplified model, we ignore the electron and neutral gas. We also ignore the self-induction magnetic field and thus the magnetic field **B** =0 in equation (1). For the ion velocity, we assume that they have the initial constant energy T_i(2eV) with arbitrary velocity component. They can be given by:

$$\begin{aligned} v_{imid} &= \sqrt{3kT_i/m} \\ v_{iz} &= v_{imid}\cos\left(2\pi R_1\right)\sin\left(2\pi R_2\right) \\ v_{ir} &= v_{imid}\cos\left(2\pi R_1\right)\cos\left(2\pi R_2\right) \\ v_{i\theta} &= v_{imid}\sin\left(2\pi R_1\right) \end{aligned} \tag{3}$$

Where R1 and R2 represent the two random number between the (0, 1). For the number of ions, the electric field is given and we consider the IEDF. Thus the ion spilling quantity didn't have much effect on the calculation results.

In this numerical model, the electric potential solutions no longer rely on the poisson equation. A set of plasma potentials over a two dimensional (r,z) space are input from the floating emissive probe. Both the average plasma potential values and time-resolved plasma potential from the waveform of potential oscillations are used to estimate the electric field, E(V/m), at each (r,z) location. The electric fields are necessary to calculate basic ion trajectories through the simulation region. Those initial potentials and electric fields could be later modified to alter the resulting ion distribution. The potential oscillations are expected to have an effect on the energy of ions observed in the distribution. For example, it is reasonable to imagine that the energetic ions originated from ions produced when the local plasma potential was at the higher points of the oscillation cycle. Otherwise the ion production rate would also likely change as a result of potential oscillations.

The plasma potential was observed to vary as a function of time and position. In general, For each (r,z) location in the simulation the potential at a given position was calculated as the average potential at that location plus an oscillation potential. We used an idealized approach to emulate the oscillations, and that is augmenting averaged value with a pure sinusoid as follows:

$$\varphi_p(r) = \bar{\varphi}_p(r) + A\sin\left(\frac{2\pi}{T}r\right)$$

Where $\bar{\varphi}_p(r)$ is the average potential at each (r,z) location, A is the amplitude factor and T is the period used to specify the frequency of the sinusoid. All the date was found directly from emissive probe measurements.

The simulation region consisted of a two dimensional array with limits is similar to the measured emissive probe regions in each case. The boundary condition is boundary fixed potential boundary.

V. Numerical Results and Discussion

Table 1 is simulation conditions for the average electric field from experimental measurement and Table 2 is simulation conditions based on the condition R5a which add oscillation potential. At the same time, in order to study how the amplitude of plasma potential oscillation and the frequency of plasma potential oscillation influence the ion energy. In the simulation conditions in table 2, we increase the amplitude of plasma potential oscillation from double amplitude to three times, and the frequency of plasma potential oscillation from ten times to one hundred times.

Table 1. simulation conditions for the average electric field

ring-type anode	Current(A)	Voltage(V)	Flow rate(sccm)
R3a	3	41.3	2.5
R5a	5	66	2.5
R9c	9	24.1	7.5

Table 2 simulation conditions for the time-resolved electric field

simulation condition（R5a）	Amplitude	Frequency
R5a(1*A*)	One time	One time
R5a(2*A*)	Two times	One time
R5a(3*A*)	three times	One time
R5a(10f)	Two times	Ten times
R5a(100f)	Two times	One hundred times

Figure 6 shows the simulation results of Ion Energy Distribution Function corresponding to the simulation conditions in table 1. The ion energy distribution is between 0~35eV and there are no high energy ions. The ion energy mainly influence by the anode discharge voltage.

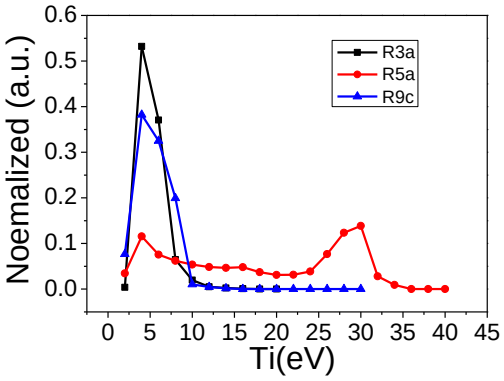

Figure 6 Ion Energy Distribution Function for the ring-type anode

Figure 7 shows the simulation results of Ion Energy Distribution Function for the ring-type anode corresponding to the simulation conditions in table 2 which add oscillation potential. The ion energy distribution is between 0~130eV and ion energy is much higher than simulation conditions in table 2 under average potential electric field. In figure 7(a) the ion energy increased as the amplitude of plasma potential oscillation increased. The maximum ion energy increased from 65eV to 103eV. In figure 7(b) the ion energy increased as the frequency of plasma potential oscillation increased. The maximum ion energy increased from 84eV to 103eV.

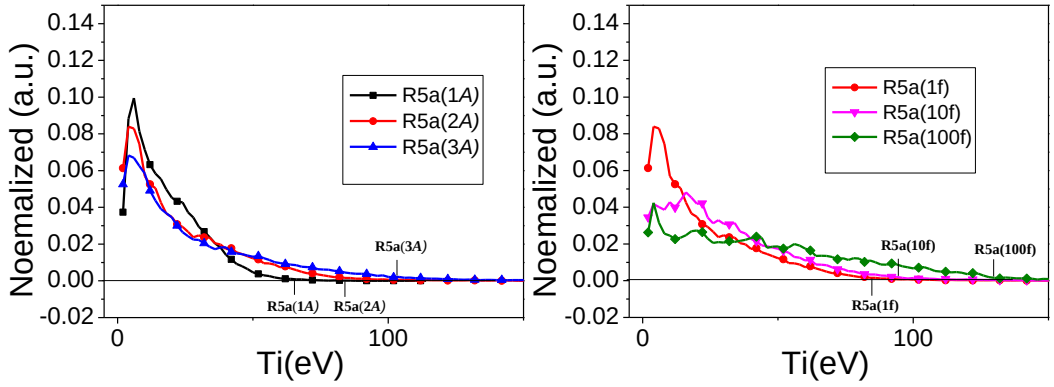

（a）changes in the amplitude　　（b）changes in the frequency

Figure 7 Ion Energy Distribution Function under potential oscillations electric field

Therefore the plasma oscillation with high amplitude and/or high frequency near the hollow cathode could produce these energetic ions which will result in energetic ions flowing toward the keeper, and eroding the electrode surfaces.

VI. Conclusion

The potential oscillations near the hollow cathode of an ion thruster are experimentally investigated. A simplified PIC numerical model that uses measurements as inputs is presented and used to investigate ion energy distribution function. The results show that at low current, the potential oscillations concentrated on the ionization-like instabilities with characteristics of low frequency and high amplitude. At high current, the potential oscillations frequency increased and the high frequency potential oscillations appears which is driven by ion acoustic turbulence with characteristics of high frequency and low amplitude. The onset of ion acoustic turbulence is observed as current increased. At high current, the potential oscillations are both driven by ionization-like instabilities and ion acoustic turbulence. The ion energy increased as the amplitude of plasma potential oscillation and the frequency of plasma potential oscillation increased by numerical simulation.

Acknowledgments

This work was supported by the National Science Foundation of China under Grant Nos.11402025 and 11475019. The authors would like to acknowledge financial support from National key laboratory of Science and Technology on Vacuum Technology &Physics under Grant no. ZWK1608.

References

[1] Vancil, B., Lorr, J., Schmidt, V., Ohlinger, W., & Polk, J. (2016). Reservoir Hollow Cathode for Electric Space Propulsion. IEEE Transactions on Electron Devices, 63(10), 4113-4118.

[2] Chu, E., & Goebel, D. M. (2012). High-current lanthanum hexaboride hollow cathode for 10-to-50-kW Hall thrusters. IEEE Transactions on Plasma Science, 40(9), 2133-2144.

[3] Xie K, Martinez R A, Williams J D 2014 Current–voltage characteristics of a cathodic plasma contactor with discharge chamber for application in electrodynamic tether propulsion *J. Phys. D: Appl. Phys.* **47(15)** 155501

[4]Zhang, T. (2013).The electric propulsion development in LIP. In IEPC2013-48, International Eelectric Propulsion Conference, The George Washington University, USA.

[5]Yanes X, Polk J. Ion Acoustic Turbulence and Ion Energy Measurements in the Plume of the HERMeS Thruster Hollow Cathode[C]//52nd AIAA/SAE/ASEE Joint Propulsion Conference. 2016: 5028.

[6]Qin Y, Xie K, Guo N, et al. The analysis of high amplitude of potential oscillations near the hollow cathode of ion thruster[J]. Acta Astronautica, 2017, 134: 265-277.

[7] Goebel D M, Jameson K, Katz I, et al. Energetic ion production and electrode erosion in hollow cathode discharges[J]. 2005.

[8] Goebel, D., Jameson, K., Katz, I., and Mikellides, I., "Plasma Potential Behavior and Plume Mode Transitions in Hollow Cathode Discharges," International Electric Propulsion Conference, IEPC Paper 2007-277, Sept. 2007.

[9] Goebel, D. M., Jameson, K. K., Katz, I., and Mikellides, I. G., "Potential fluctuations and energetic ion production in hollow cathode discharges," Physics of Plasmas, Vol. 14, No. 10, 2007.

[10]Boeuf J P, Garrigues L. Low frequency oscillations in a stationary plasma thruster[J]. Journal of Applied Physics, 1998, 84(7): 3541-3554.

[11] Grubisic, Angelo N., and Stephen B. Gabriel. "Assessment of the T5 and T6 Hollow Cathodes as Reaction Control Thrusters." *Journal of Propulsion and Power* (2016): 1-11.

[12]Jorns B A, Mikellides I G, Goebel D M. Ion acoustic turbulence in a 100-A LaB 6 hollow cathode[J]. Physical Review E, 2014, 90(6): 063106.

[13]Jorns B A, Mikellides I G, Goebel D M. Investigation of energetic ions in a 100-a hollow cathode[J]. 2014.

[14]Jorns B A, Mikellides I G, Goebel D M. Temporal fluctuations in a 100-A LaB6 hollow cathode[C]//Proceedings of the 33rd International Electric Propulsion Conference, Washington, DC. 2013: 2013-385.